Journal of Molecular Catalysis A: Chemical 310 (2009) 166–173

Contents lists available at ScienceDirect

Journal of Molecular Catalysis A: Chemical

journal homepage: www.elsevier.com/locate/molcata

Vapor-phase catalytic reactions of alcohols over bixbyite indium oxide

Masaki Segawa [a], Satoshi Sato [a,*], Mika Kobune [a], Toshiaki Sodesawa [a], Takashi Kojima [a], Shin Nishiyama [a], Nobuo Ishizawa [b]

[a] Graduate School of Engineering, Chiba University, Yayoi, Inage, Chiba 263-8522, Japan
[b] Nagoya Institute of Technology, Tajimi, Gifu 507-0071, Japan

ARTICLE INFO

Article history:
Received 20 March 2009
Received in revised form 12 June 2009
Accepted 13 June 2009
Available online 24 June 2009

Keywords:
Dehydration
In_2O_3
3-Buten-1-ol
1,4-Butanediol
4-Penten-1-ol
1,5-Pentanediol

ABSTRACT

Vapor-phase catalytic reactions of several alcohols were investigated over In_2O_3. In_2O_3 showed stable catalytic activity in the dehydration of terminal diols, such as 1,4-butanediols and 1,5-pentanediol, to produce unsaturated alcohols, such as 3-buten-1-ol and 4-penten-1-ol, respectively, with selectivities higher than 70 mol%. Although the dehydration of 1,3-diols, such as 1,3-propanediol and 1,3-butanediol, also proceeded over In_2O_3, the catalytic activity decreased with time on stream because of dehydrogenation followed by retro aldol reaction of the resulting dehydrogenated products. In contrast, in the reaction of monoalcohols, such as 1-butanol and 2-octanol, dehydrogenation dominantly proceeded to produce butanal and 2-octanone, respectively. Although In_2O_3 has cubic bixbyite crystal structure that is the same as those of heavy rare earth oxides, the catalytic activity of In_2O_3 was similar to that of cubic fluorite CeO_2 with redox property, rather than those of heavy rare earth oxides with acid–base property. Redox sites of In_2O_3 are concluded to be active centers for the dehydration of diols to produce unsaturated alcohols.

1. Introduction

We have previously reported that several rare earth oxides (REOs), such as CeO_2, Er_2O_3, and Yb_2O_3, were effective for the dehydration of diols, such as 1,3- and 1,4-butanediols, to produce unsaturated alcohols [1–12]. CeO_2 catalyzes the dehydration of 1,3-diols into unsaturated alcohols [1–6]: 3-buten-2-ol and *trans*-2-buten-1-ol are produced from 1,3-buanediol at 325 °C with selectivities of 57 and 36 mol%, respectively [2]. In the dehydration of 1,4-butanediol over CeO_2 at 400 °C, 3-buten-1-ol is produced with maximum selectivity of 68 mol% [7]. The dehydration of butanediols is a surface-structure-sensitive reaction: active sites are located on the (1 1 1) facets of CeO_2 surface [3–6].

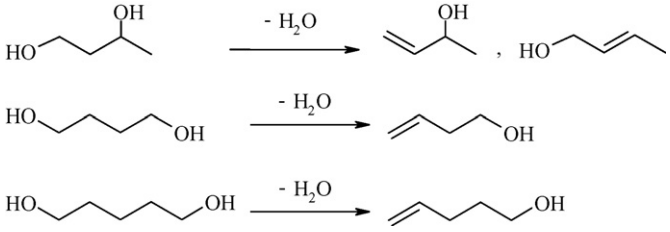

Heavy REO catalysts, such as Tb_4O_7, Er_2O_3, Tm_2O_3, Yb_2O_3, Lu_2O_3, and Y_2O_3, are selective for the production of 3-buten-1-ol from 1,4-butanediol [8,12]: the selectivity to 3-buten-1-ol exceeds 80 mol%, together with the formation of tetrahydrofuran (THF). In the reaction of 1,4-butanediol, the catalytic function of REOs is related to the basic properties of REO originated in lanthanide contraction [9]. 1,5-Pentanediol is also converted into 4-penten-1-ol with selectivity higher than 75 mol% over Yb_2O_3 [10]. The surface character of REOs is basic rather than acidic [10,13]. We have also found that Yb_2O_3 shows different catalytic activities depending on its crystal structure [8], which varies from monoclinic to cubic at temperatures around 800 °C. Yb_2O_3 supported on monoclinic zirconia is also active for the selective formation of 3-buten-1-ol from 1,4-butanediol [11]. We should notice that heavy REOs with the cubic bixbyite structure shows high formation rate of 3-buten-1-ol [12,13].

On the other hand, there are a few studies on the catalytic property of In_2O_3. In_2O_3 is selective for the formation of 1-alkenes from 2-alcohols [14,15]. This feature resembles those of REOs [16–18]. In_2O_3 is also active for dehydrogenation as well as dehydration, and the surface of In_2O_3 is reduced by alcohols [14]. The reduction of In_2O_3 is limited within a few surface layers [19]. It is recently reported that pure In_2O_3 is also active in the hydrogen production, such as methane decomposition [20] and steam reforming of alcohols [21,22]. In_2O_3 has cubic bixbyite structure that is the same as that of C-type REOs [23], which are active for the dehydration of diols to produce unsaturated alcohols [8,12]. Accordingly, we expect that In_2O_3 would have similar catalytic activity of Yb_2O_3.

In this paper, we investigated catalytic activity of pure In_2O_3 for the reactions of several alcohols. We also performed the

* Corresponding author. Tel.: +81 43 290 3376; fax: +81 43 290 3401.
E-mail address: satoshi@faculty.chiba-u.jp (S. Sato).

1381-1169/$ – see front matter © 2009 Elsevier B.V. All rights reserved.
doi:10.1016/j.molcata.2009.06.015

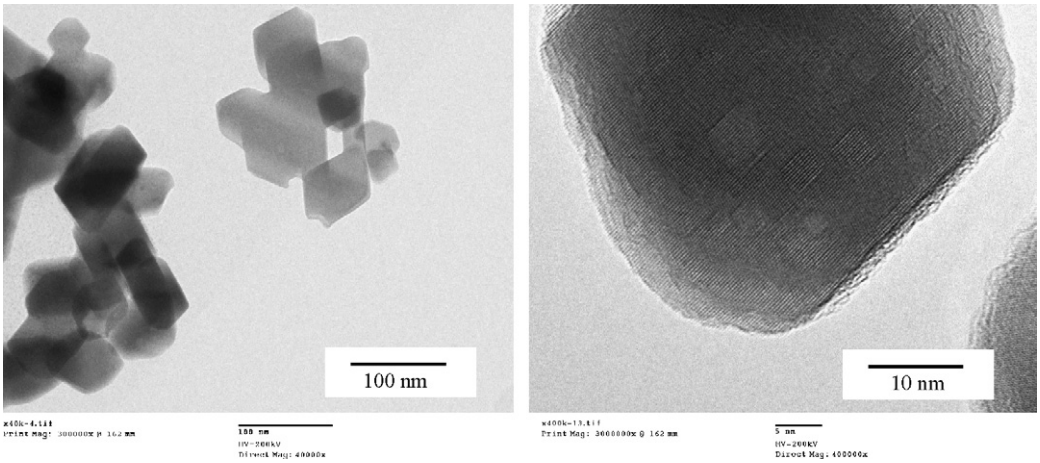

Fig. 1. TEM photographs of In_2O_3.

dehydration of 1,4-butanediol in different carrier gases to clarify the features of active sites of In_2O_3. Then, we discussed the catalytic properties of In_2O_3 in connection with the crystal structure and surface chemical properties.

2. Experimental

2.1. Samples

Reagents, such as, 1,3-propanediol, 1,3-butanediol, 1,4-butanediol, 1,5-pentanediol, 1-butanol, 2-octanol, and In_2O_3 were purchased from Wako Pure Chemical Industries, Japan. The alcohols were used for the catalytic reaction without further purification.

2.2. Catalytic reaction

The catalytic reactions were performed in a fixed-bed down-flow reactor with the inside diameter of 17 mm. Prior to the reactions, an In_2O_3 sample (weight, $W = 0.50$ g) was preheated in the reactor in N_2 flow at 500 °C for 1 h. After the temperature of catalyst bed was set at a prescribed temperature between 300 and 375 °C, a reactant was fed through the reactor top at a liquid feed rate, F, of 2.67 $cm^3\,h^{-1}$ together with N_2 flow of 30 $cm^3\,min^{-1}$. The effluent collected at −77 °C every hour was analyzed by gas chromatography (GC-8A, Shimadzu, Japan) with a flame ionization detector and a 30-m capillary column (TC-WAX, GL Science Inc., Japan) and by gas chromatography with a mass spectrometer (GCMS-QP-5050A, Shimadzu, Japan) and a 30-m capillary column (DB-WAX, Agilent Technologies, USA). In this paper, the catalytic activity was evaluated by averaging the conversion data in the initial 5 h of time on stream irrespective of catalyst deactivation. The conversion of alcohol is defined as the amount of alcohol consumed in the reaction. The selectivity to each product is defined as molar selectivity.

We carried out the reactions of 1,4-butanediol and 2-octanol in different carrier gases in order to elucidate the catalytic functions of In_2O_3. In the experiment, instead of N_2 carrier gas, either CO_2 or H_2 was used at 30 $cm^3\,min^{-1}$. An equimolar mixture of NH_3 and N_2 at the total flow rate of 30 $cm^3\,min^{-1}$ was also used as a carrier gas.

2.3. Characterization of catalyst

The specific surface area of the catalyst, SA, was calculated with the BET method using N_2 isotherm at −196 °C. The SA of In_2O_3 was 6.7 $m^2\,g^{-1}$. X-ray diffraction (XRD) patterns were recorded on an M18XHF (Mac Science, Japan) using CuK_α radiation ($\lambda = 0.15$ nm) to detect the crystal structure of the samples. Transmission electron microscopy (TEM, JEM-2010, JEOL) was employed to observe the morphology of crystallites of In_2O_3. Average particle size of In_2O_3, D, was calculated by the following equation, assuming that the particles are spherical: $D = 6/d\,SA$, where d is the density of In_2O_3 ($d = 7.18$ g cm^{-3} [24]).

Temperature-programmed desorption (TPD) of adsorbed NH_3 as well as CO_2 was examined by neutralization titration using an electric conductivity cell immersed in aqueous solution, as has been described elsewhere [25–27]. NH_3 and CO_2 that desorbed with N_2 carrier gas were bubbled into a dilute H_2SO_4 and NaOH solution, respectively. The catalyst sample was heated from 25 to 800 °C at a rate of 10 K min^{-1} in N_2 flow. The amount of desorbed NH_3 or CO_2 was monitored from the change in conductivity of the solution.

Temperature-programmed reduction (TPR) measurement was done from 25 to 900 °C at a heating rate of 5 K min^{-1}, and the details are described elsewhere [28]. A mixture of H_2/N_2 (=1/9) was flowed at a flow rate of 10 $cm^3\,min^{-1}$ and ambient pressure over the catalyst sample filled in a quartz tube. The amount of H_2 consumed for the reduction of sample was monitored with a thermal conductivity detector.

3. Results

3.1. Characterization of In_2O_3

The diffraction pattern of In_2O_3 (pattern not shown) is assigned to bixbyite sesquioxide [29], which is the same as C-type cubic REOs [8,13,23]. Fig. 1 shows TEM photographs of In_2O_3. In the TEM photograph, In_2O_3 particles with flat surfaces were dominant and some of them had a shape with tetragonal bipyramidal. The crystallites seemed to expose most of their outer surfaces. Particles of ca. 50–100 nm were observed in the In_2O_3 sample.

Fig. 2a shows the TPR profile of In_2O_3 measured up to 900 °C. Two reduction peaks were observed at around 200 and 700 °C. The large peak at ca. 700 °C is assigned as the reduction of bulk In_2O_3. In_2O_3 was reduced to indium metal after TPR experiment, which is confirmed by XRD measurement (profile not shown). The other peak at ca. 200 °C is attributed to the reduction of surface In_2O_3 [14]. It was confirmed that color of In_2O_3 turned from yellow to brown. Fig. 2b and c shows TPD profiles of NH_3 and CO_2 adsorbed on In_2O_3, respectively. There were no peaks and the acidic and basic gases were not adsorbed.

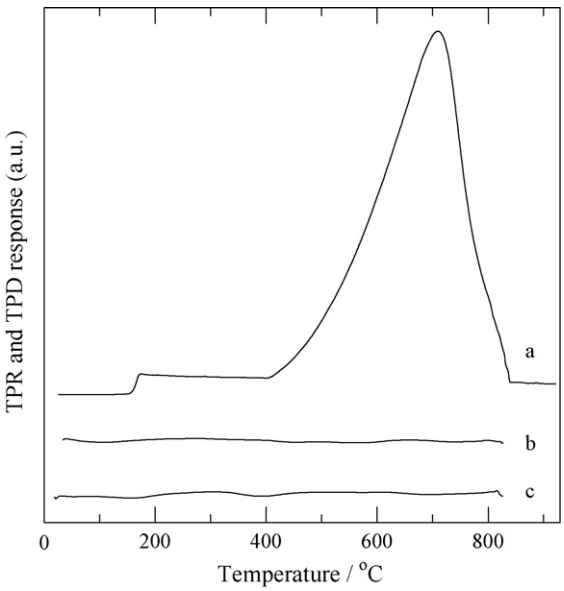

Fig. 2. (a) TPR profile of In_2O_3 and TPD profiles of (b) NH_3 and (c) CO_2 adsorbed on In_2O_3.

3.2. Catalytic reactions of alcohols over In_2O_3

Fig. 3 shows the change in the catalytic activity of In_2O_3 with time on stream in the dehydration of 1,3-propanediol at 375 °C. The conversion steeply decreased with time on stream. Table 1 summarizes average catalytic activity of In_2O_3 for 1,3-propanediol at temperatures of 300–375 °C. The average conversion increased with increasing reaction temperature. The selectivity to 2-propen-1-ol was higher than 90 mol%. Dehydration of 1,3-propanediol proceeded dominantly, while major by-products were 2-propenal and acetaldehyde.

In the reaction of 1,3-butanediol, deactivation in the conversion was also observed in a similar way to 1,3-propanediol shown in Fig. 3. Table 2 shows the average catalytic activity of In_2O_3 for 1,3-butanediol. The average conversion increased with increasing the reaction temperature. The products were 3-buten-2-ol, 2-buten-1-ol, 3-buten-1-ol, acetone, acetaldehyde and 3-buten-2-one. The total selectivity for dehydration products, such as 3-buten-2-ol, 2-buten-1-ol and 3-buten-1-ol, was 83.9 mol% at 300 °C. By-products, such as acetaldehyde and 3-buten-2-one, increased with increasing reaction temperature.

Table 1
Catalytic conversion of 1,3-propanediol over In_2O_3[a].

RT (°C)	Conversion (%)	Selectivity (mol%)			
		2-Propen-1-ol	2-Propenal	AcH	Others
300	11.4	93.4	4.7	0.1	1.2
325	26.6	92.8	5.6	0.9	0.7
350	34.5	93.1	4.5	1.2	1.2
375	48.9	90.1	5.2	1.4	3.3

[a] RT, reaction temperature. Conversion and selectivity were averaged in the initial 5 h. $W/F = 0.187$ g h cm^{-3} where W and F are catalyst weight and flow rate of reactant fed, respectively. N_2 carrier flow rate = 30 cm^3 min^{-1}. AcH, acetaldehyde; others contain 1-propanol and several unknown products.

Fig. 4 depicts the changes in catalytic activity of In_2O_3 with time on stream in the dehydration of 1,4-butanediol at 375 °C. No deactivation in the conversion was observed. Table 3 summarizes the catalytic conversion of 1,4-butanediol over In_2O_3 at 300–375 °C. Conversion of 1,4-butanediol was increased with increasing reaction temperature. The highest selectivity to 3-buten-1-ol, which is a dehydrated product, was 71.4 mol% at 325 °C. Major by-product was γ-butyrolactone, which is a dehydrogenated product.

In the reaction of 1,5-pentanediol over In_2O_3, no deactivation was observed even at 375 °C (figure not shown). Table 4 lists average conversion and selectivity in the reaction of 1,5-pentanediol over In_2O_3. The conversion of 1,5-pentanediol was increased with increasing reaction temperature. The major product was 4-penten-1-ol, which is a dehydration product. The highest selectivity to 4-penten-1-ol was 70.8 mol% at 350 °C. Major by-products were tetrahydropyran and δ-valerolactone, which are dehydrated and dehydrogenated products, respectively. In the reactions of 1,3-propanediol, 1,3-butanediol, 1,4-butanediol and 1,5-pentanediol, the selectivity to the corresponding unsaturated alcohol exceeds 70% while no further dehydration into dienes proceeded over In_2O_3 (Tables 1–4). At high temperatures, the unsaturated alcohols were hydrogenated and

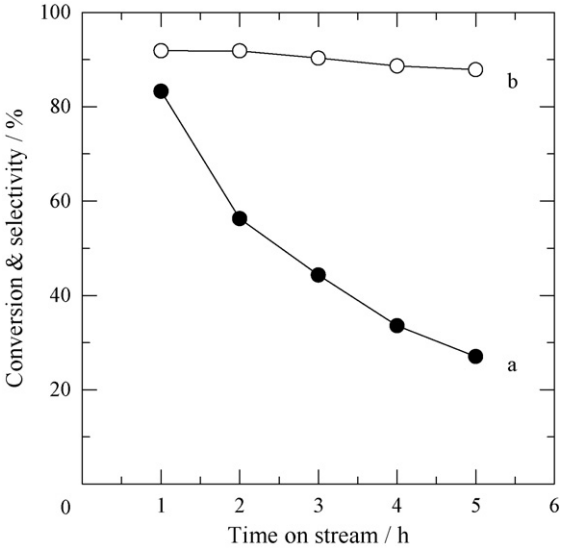

Fig. 3. Changes in conversion and selectivity in the dehydration of 1,3-propanediol over In_2O_3 at 375 °C with time on stream. (a) Solid circle, conversion of 1,3-propanediol; (b) open circle, selectivity to 2-propen-1-ol. $W/F = 0.187$ g h cm^{-3}, N_2 carrier gas flow rate = 30 cm^3 min^{-1}.

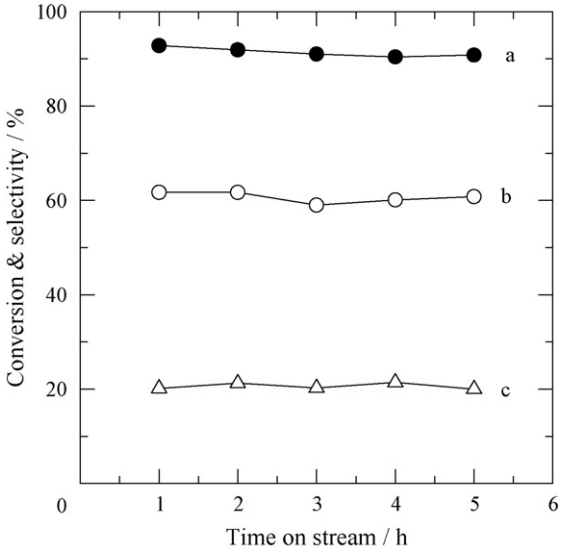

Fig. 4. Changes in conversion and selectivity in the dehydration of 1,4-butanediol over In_2O_3 at 375 °C with time on stream. (a) Solid circle, conversion of 1,4-butanediol; (b) open circle, selectivity to 3-buten-1-ol; (c) triangle, selectivity to γ-butyrolactone. $W/F = 0.187$ g h cm^{-3}.

Table 2
Catalytic conversion of 1,3-butanediol over In_2O_3[a].

RT (°C)	Conversion (%)	Selectivity (mol%)									
		Dehydrogenated products				Dehydrated products					Others
		AcH	Acetone	MVK	Sum	3B2ol	3B1ol	t2B1ol	c2B1ol	Sum	
300	18.5	0.0	0.0	13.7	13.7	25.0	22.4	28.7	7.8	83.9	2.4
325	48.8	0.0	0.0	11.9	11.9	32.9	13.8	29.4	5.3	81.4	6.6
350	57.1	1.3	4.7	13.9	19.9	30.2	15.3	22.5	6.3	74.3	5.8
375	87.1	1.9	8.4	16.6	26.9	32.7	9.0	16.3	4.3	62.3	10.8

[a] Reaction conditions are the same as those in Table 1. Conversion and selectivity were averaged in the initial 5 h. AcH, acetaldehyde; MVK, 3-buten-2-one; 3B2ol, 3-buten-2-ol; 3B1ol, 3-buten-1-ol; c2B1ol, *cis*-2-buten-1-ol, t2B1ol, *trans*-2-buten-1-ol. Other by-products are 1-butanol, 2-butanol, and several unknown products.

Table 3
Catalytic conversion of 1,4-butanediol over In_2O_3[a].

RT (°C)	Conversion (%)	Selectivity (mol%)						
		3B1ol	t2B1ol	c2B1ol	THF	GBL	1-Butanol	Others
300	23.6	55.6	0	0	5.6	22.8	0.2	15.9
325	42.2	71.4	0.9	0.7	3.6	17.7	0.3	5.5
350	65.3	64.9	0.6	0.3	4.9	20.4	1.1	7.8
375	91.3	60.8	0.2	0.2	4.8	20.4	2.3	11.4
325[b]	41.3	66.6	0.1	0	2.4	20.1	0.4	10.3
325[c]	24.5	59.0	0.9	0.7	1.1	30.6	0.3	7.6
325[d]	23.2	56.2	0	0	3.7	20.2	0.1	19.8
325[e]	40.9	66.8	0.4	0.4	1.8	23.2	0.6	6.7
325[e,f]	15.0	21.9	0	0	0.8	34.1	0.6	42.7

[a] Reaction conditions are the same as those in Table 1. Conversion and selectivity were averaged in the initial 5 h. Total flow rate of carrier gas was 30 cm^3 min^{-1}. THF, tetrahydrofuran; 3B1ol, 3-buten-1-ol; t2B1ol, *trans*-2-buten-1-ol; c2B1ol, *cis*-2-buten-1-ol; GBL, γ-butyrolactone. Others contain butanal and several unknown products.
[b] CO_2 was used as carrier gas.
[c] An equimolar mixture of NH_3 and N_2 was used as carrier gas.
[d] N_2 was used as carrier gas after the In_2O_3 sample had been preheated in an equimolar mixture of NH_3 and N_2 at 325 °C for 1 h prior to the reaction.
[e] H_2 was used as carrier gas.
[f] The In_2O_3 sample was reheated in H_2 at 450 °C for 1 h prior to the reaction.

dehydrogenated to produce saturated alcohols and aldehydes, respectively.

In the reactions of 1-butanol and 2-octanol over In_2O_3, no deactivation was observed (figures not shown). Table 5 summarizes the results of 1-butanol conversion over In_2O_3. Major products were butanal, 1-butene, and butyl butanoate. The selectivity to butanal, which is a dehydrogenated product, was higher than 50 mol% and the selectivity to 1-butene was lower than 15 mol%. The dehydrogenation preferentially proceeded at higher temperatures, and the selectivity to butanal reached 87.2 mol% at 375 °C.

Table 6 shows the conversion of 2-octanol over In_2O_3. Dehydrogenation is the primary reaction: the selectivity to 2-octanone was over 80 mol%. The selectivity to the sum of dehydrated products, such as 1-octene, *trans*-2-octene, and *cis*-2-octene, was below 10 mol%. 1-Octene formed by Hofmann elimination was the major product with minor products of 2-octenes. Produced octene ratios, which are 1-/2-octene and *trans*-2-/*cis*-2-octene, did not vary significantly with the reaction temperature. Dehydrogenation is preferential in the reaction of monoalcohols over In_2O_3, in contrast to the reaction of diols, such as 1,4-butanediol and 1,5-pentanediol.

Table 4
Catalytic conversion of 1,5-pentanediol over In_2O_3[a].

RT (°C)	Conversion (%)	Selectivity (mol%)				
		4-Penten-1-ol	THP	DVL	1-Pentanol	Others
300	9.7	53.4	8.6	16.3	0.0	21.7
325	16.6	63.5	7.7	15.4	1.1	12.3
350	36.9	70.8	5.4	11.1	1.1	11.5
375	57.3	67.4	7.0	12.7	2.6	10.3

[a] Reaction conditions are the same as those in Table 1. Conversion and selectivity were averaged in the initial 5 h. THP, tetrahydropyran; DVL, δ-valerolactone. Others contain pentanal and several unknown products.

Table 5
Catalytic conversion of 1-butanol over In_2O_3[a].

RT (°C)	Conversion (%)	Selectivity (mol%)				
		1-Butene	Butanal	Butyl butanoate	Butanoic acid	Others
300	3.1	13.1	53.5	29.7	1.5	2.2
325	10.0	12.9	58.5	26.8	0.6	1.2
350	17.0	10.3	62.0	23.8	1.4	2.5
375	21.0	2.1	87.2	7.8	1.6	1.4

[a] Reaction conditions are the same as those in Table 1. Conversion and selectivity were averaged in the initial 5 h. Others contain 1-butanol and several unknown products.

3.3. Catalytic activity of In_2O_3 for alcohols in different atmospheres

Table 3 also summarizes catalytic conversion in the dehydration of 1,4-butanediol over In_2O_3 at 325 °C in different carrier gases. CO_2, NH_3, and H_2 were used as a carrier gas instead of N_2. In CO_2 and H_2 flows, the yield of 3-buten-1-ol was not affected at 325 °C. In contrast, the yield of 3-buten-1-ol in NH_3 was reduced to ca. 3/5 of that in N_2 flow. The adverse effects of NH_3 seem to indicate that active sites are poisoned by NH_3, which means that acidic sites may be the active sites. However, NH_3 poisons the catalyst surface irreversibly: the catalytic activity of In_2O_3 was not recovered after being switched back in N_2 flow. The poisoning effect was high in the contact of In_2O_3 with the reductive gases at higher temperatures: the contact with NH_3 at 500 °C completely deactivated the surface of In_2O_3 (data not shown). The contact of In_2O_3 surface with the

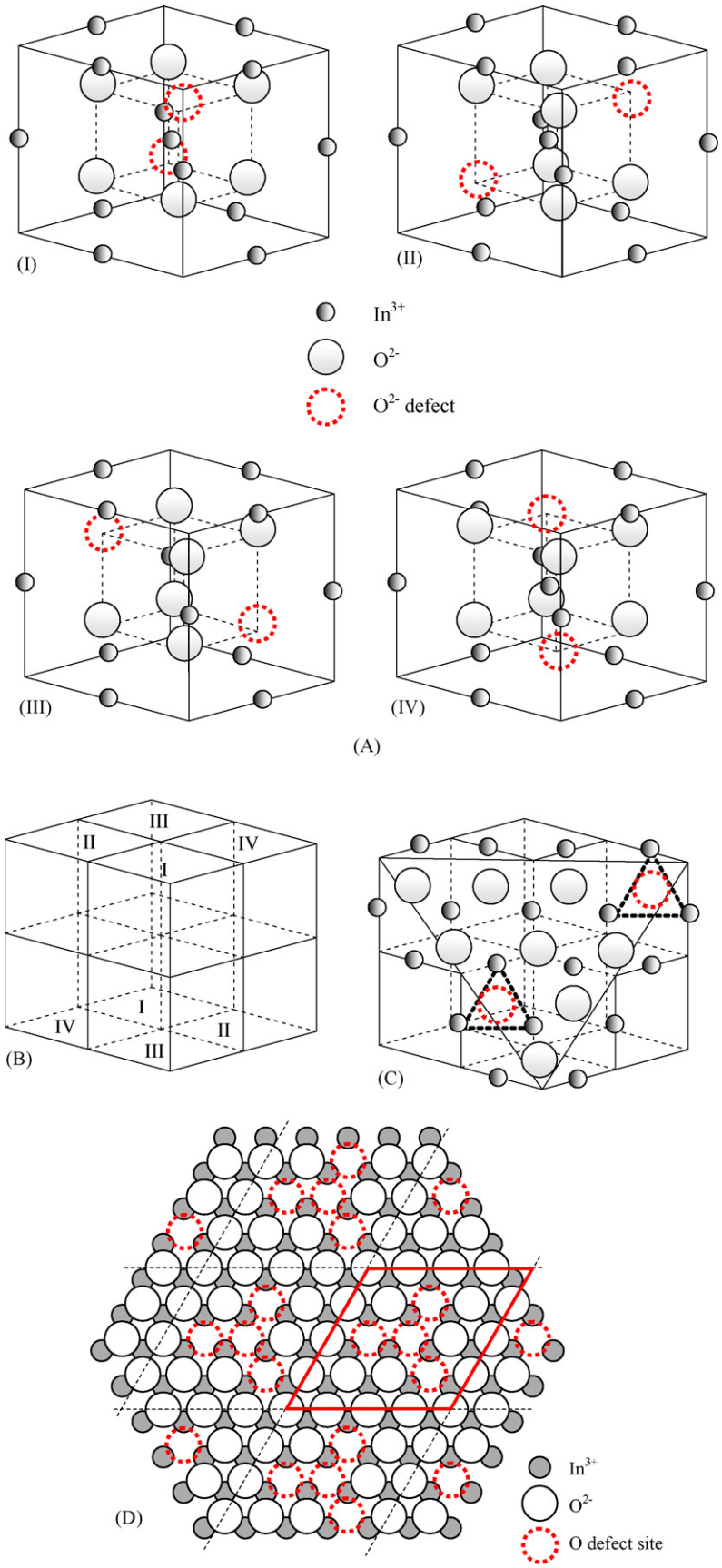

Fig. 5. Crystal structure of In_2O_3. (A) Subunits of octant types I–IV, (B) unit cell, (C) and (D) (2 2 2) plane of In_2O_3. The triangle shows a surface oxygen defect site.

Table 6
Catalytic conversion of 2-octanol over In_2O_3[a].

RT (°C)	Conversion (%)	Selectivity (mol%)					Ratio of butenes	
		1-Octene	t2Oe	c2Oe	2-Octanone	Others	1-/2-	t-/c-
300	26.4	17.4	1.6	0.4	79.2	1.5	8.6	4.1
325	60.7	15.5	1.2	0.3	82.2	0.9	10.3	4.0
350	75.8	13.7	1.4	0.3	84.5	0.1	8.5	5.2
375	95.5	8.9	0.9	0.2	89.7	0.3	8.2	3.9
325[b]	55.7	23.6	1.9	0.5	71.9	2.2	9.8	3.8
325[c]	5.4	12.1	0.6	0.1	56.4	30.8	17.3	6.0
325[d]	61.1	16.6	1.3	0.3	80.8	1.0	10.4	4.3
325[d,e]	53.2	19.0	1.3	0.3	78.2	1.3	11.9	4.3

[a] Reaction conditions are the same as those in Table 3. Conversion and selectivity were averaged in the initial 5 h. t2Oe, *trans*-2-octene; c2Oe, *cis*-2-octene. 1-/2-, 1-butene/2-butenes; t-/c-, *trans*-2-octene/*cis*-2-octene. Others are several unknown products.
[b] CO_2 was used as carrier gas.
[c] An equimolar mixture of NH_3 and N_2 was used as carrier gas.
[d] H_2 was used as carrier gas.
[e] The catalyst sample was reheated in H_2 at 500 °C for 1 h prior to the reaction.

reductive gases such as NH_3 and H_2 may induce the reduction of In_2O_3. This could be related to the reduction peak in the TPR profile depicted in Fig. 2a.

Table 6 also summarizes conversion and selectivity in the dehydrogenation of 2-octanol over In_2O_3 at 325 °C in different carrier gases, such as CO_2, NH_3, and H_2. In CO_2 and H_2 flows, the yield of 2-octanone was not affected whereas that in NH_3 flow was reduced to ca. 1/10 of that in N_2 flow. The effects of carrier gases on the catalytic reaction of 2-octanol are essentially the same as those of 1,4-butanediol. The major reaction is dehydrogenation to 2-octanone, so that the reaction produces H_2. It is quite reasonable that H_2 gas did not work as poison at 325 °C.

4. Discussion

4.1. Structural and surface properties of In_2O_3

We have previously reported that CeO_2 works as an excellent catalyst for the dehydration of butanediols [1–7]. The crystal structure of CeO_2 is cubic fluorite where Ce^{4+} has 8 coordination and O^{2-} has 4 coordination. The most stable face of CeO_2 is (1 1 1) plane [5,30] and an oxygen defect of the surface is the active site for the dehydration of diols [3,4]. The cubic bixbyite structure of In_2O_3 as well as Yb_2O_3 is a fluorite-related structure [13,31–33]. A subunit of bixbyite is the same as the unit cell of fluorite. The difference between the structures is that a subunit of bixbyite has two oxygen defects. There are 4 different subunits, octant types I–IV (Fig. 5A), which are packed regularly in a cube to form bixbyite unit cell as Fig. 5B. Thus, the unit cell volume is 8 times larger than that of fluorite. The most stable face of bixbyite would be (2 2 2) plane, as shown in Fig. 5C. Oxygen defects with exposed three In^{3+} are located on the (2 2 2) plane as depicting triangle in Fig. 5C. On a large (2 2 2) plane depicted in Fig. 5D, a quarter of oxygen anion sites are vacant like an asterism, which is regularly located on the plane exposing nine In^{3+} cations.

The average particle size of In_2O_3, D, is calculated by using SA value of 6.7 $m^2\,g^{-1}$ to be 125 nm. The calculated D value is larger than the crystallite size observed in TEM photograph (Fig. 1). The difference between the values is explained by the fact that the particles observed in TEM are fused with each other. Thus, this indicates that the crystallites are non-porous and that most of the crystallite surfaces are exposed. As shown in Fig. 1, some In_2O_3 particles have tetragonal bipyramidal shape. A similar photograph is reported in Ref. [34]. The surface on the tetragonal bipyramidal shape is the most stable (2 2 2) face, which could provide active sites. In the Section 4.3, we discuss the reaction mechanism in the diol dehydration over In_2O_3 (2 2 2) face.

We have recently reported that the catalytic activity of Er_2O_3 is greatly reduced in CO_2 flow even at 375 °C, and that it is caused by acid–base concerted mechanism [12]. In Fig. 2b and c, TPD profiles of adsorbed NH_3 and CO_2 clearly indicate that the In_2O_3 surface is neutral in the sense of the interaction of the acidic and basic gases at an ambient temperature. In Fig. 2a, the TPR profile indicates that the surface In^{3+} cations are readily reduced by H_2 at temperatures above 200 °C. In Tables 3 and 6, the poisoning effect of CO_2 indicates that basic sites of In_2O_3 are not active centers in the reactions at 325 °C. In Table 3, NH_3 poisons the catalyst surface. The poisoning is not reversible and so it is probably caused by either the formation of nitrite or the reduction of the surface. It is known that the surface of In_2O_3 is readily reduced [14], and the reduction of In_2O_3, as well as TiO_2, Cr_2O_3, ZnO, SnO_2, and WO_3, is limited within a few surface layers [19]. Therefore, the In_2O_3 surface has redox property rather than acid–base property.

Dehydrogenation is the main reaction when monoalcohols, such as 1-butanol and 2-octanol, was reacted over In_2O_3 (Tables 5 and 6). In the reaction of 2-octanol, the distribution of octenes, i.e. 1-octene, *cis*-2-octene and *trans*-2-octene, is almost constant at temperatures between 300 and 375 °C. This indicates that no isomerization proceed over In_2O_3. Thus, it can be concluded that In_2O_3 surface is less acidic and less basic.

4.2. Catalytic activities of In_2O_3

When diols contact In_2O_3, dehydration proceeds to form unsaturated alcohols. However, deactivation behavior depends upon the reactants: catalytic deactivation was observed in the reactions of 1,3-propanediol and 1,3-butanediol. We have to notice by-products of the reactions of diols. Such lactones as γ-butyrolactone and δ-valerolactone are stable and do not poison the In_2O_3 surface (Fig. 4), which are formed in the dehydrogenation–cyclization of 1,4-butanediol and 1,5-pentanediol, respectively. On the other hand, neither β-propiolactone nor 3-hydroxypropanal are observed in the reaction of 1,3-propanediol. β-Lactone, which could be produced from 1,3-diols via dehydrogenation–cyclization, is unstable, and 3-hydroxypropanal produced by dehydrogenation of 1,3-propanediol would easily decompose into formaldehyde and acetaldehyde via retro aldol addition. Carbon deposition caused from formaldehyde would result in the catalyst deactivation of In_2O_3, as shown in Fig. 3. In the dehydration of 1,3-butanediol, 3-hydroxybutanal could be the intermediate of formaldehyde, which is formed via retro aldol addition of 3-hydroxybutanal together with the formation of acetone.

Fig. 6 compares the formation rates of unsaturated alcohols from diols with those of aldehyde/ketone from monoalcohols. The rates

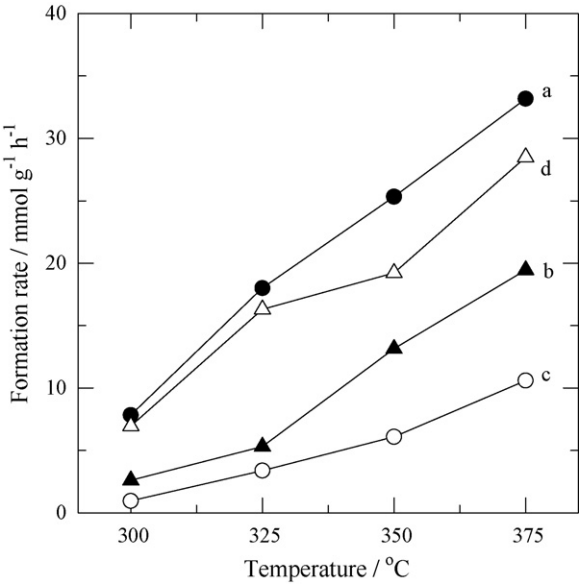

Fig. 6. Changes in the formation rate over In_2O_3 with reaction temperature. (a) Formation rate of 3-buten-1-ol from 1,4-butanediol; (b) 4-penten-1-ol from 1,5-pentanediol; (c) butanal from 1-butanol; (d) 2-octanone from 2-octanol. $W/F = 0.187$ g h cm^{-3}.

increase with increasing reaction temperature. The formation rate of 4-penten-1-ol is lower than that of 3-buten-1-ol. Although the formation rate of 2-penten-1-ol from 1,3-propanediol decreases with time on stream (Fig. 3), the initial formation rate of 2-penten-1-ol is higher than that of 3-buten-1-ol from 1,4-butanediol. The initial formation rate of dehydrated products from 1,3-butanediol is comparable to that of 2-propen-1-ol from 1,3-propanediol. In the reaction 3-buten-2-one is a dehydrogenated product from 3-buten-2-ol that is a dehydrated product (Table 2). The total selectivity to dehydrated products including 3-buten-2-one, exceeds 90% at <350 °C, and so the dehydration is the primary reaction. With increasing reaction temperature, dehydrogenation activity of In_2O_3 increased in the reaction of 1,3-butanediol. Thus, the reactivity of the diols is summarized: terminal diols with short carbon chain are more reactive than those with longer one. Then, the formation rate of 2-octanone from 2-octanol is as high as that of 3-buten-1-ol from 1,4-butanediol (Fig. 6). This indicates that the reaction rate of diol dehydration is comparable to that of 2-alcohol dehydrogenation. In the reaction of monoalcohols, dehydrogenation is preferential, and 2-octanol is more reactive than 1-butanol. Thus, the secondary OH group can be readily dehydrogenated by In_2O_3 surface.

No diene is observed in the reactions of diols. This is explained by the difference in the reactivity of alcohols. 1,3-Butadiene has to be formed through 3-buten-1-ol from 1,4-butanediol. The first step of 3-buten-1-ol formation is fast, but the second step is the dehydration of 3-buten-1-ol, which is regarded as primary monoalcohol. The dehydration of primary monoalcohol is slower than the dehydrogenation (Fig. 6). Thus, it is reasonable that no diene is produced over In_2O_3.

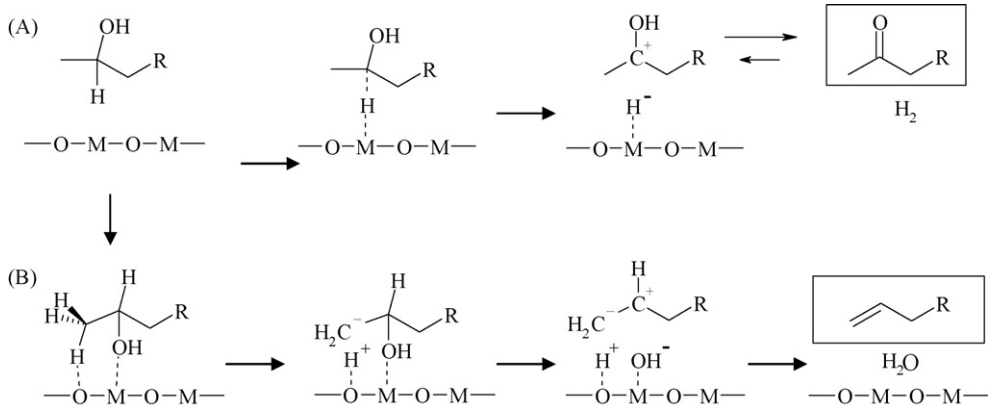

Fig. 7. Adsorption models for the dehydrogenation and dehydration of 2-octanol (R = n-C_5H_{11}).

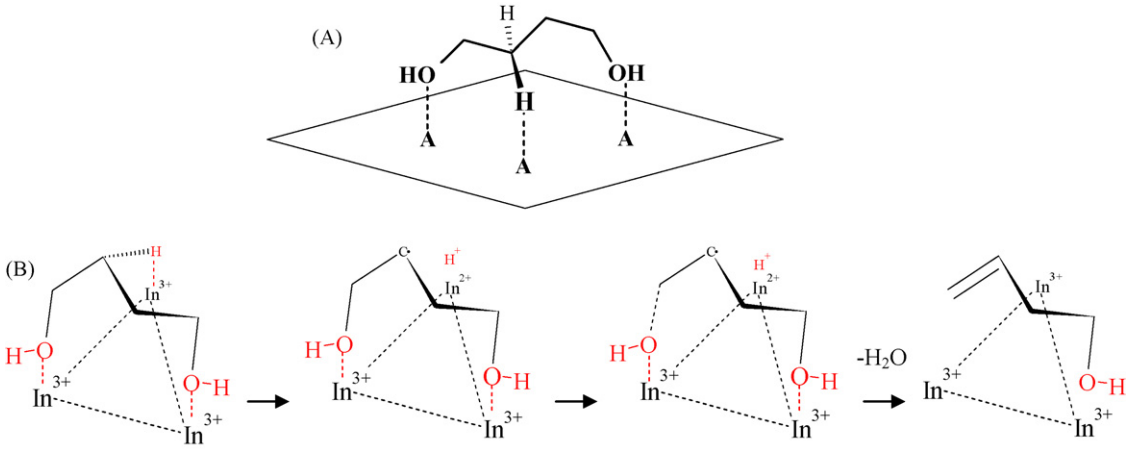

Fig. 8. (A) Probable adsorption structure of 1,4-butenediol on In_2O_3 where A is an adsorption site and (B) proposed reaction mechanism of 1,4-butenediol over In_2O_3.

4.3. Probable reaction mechanism over In_2O_3

The adsorption model of secondary alcohols on In_2O_3 has been proposed: metal and oxygen ions on catalyst are involved in the dehydration and dehydrogenation of secondary alcohols [14]. Fig. 7A depicts dehydrogenation process. First, α-position of hydrogen in 2-octanol adsorbs on a metal ion. Then, the hydrogen is extracted and the resulting enol was tautomerized to produce ketone. Fig. 7B shows dehydration process of secondary alcohol. First, β-hydrogen of 2-octanol adsorbs on an oxide anion, O^{2-}, and is extracted by basic O^{2-}. Then, α-OH in the resulting enolate coordinates to a metal ion. Finally, either 1-octene or 2-octene is produced after extraction of the OH group. The stability of enolate anion after extraction of β-hydrogen explains the results that the selectivity to 1-octene was higher than that of 2-octene. Dehydrogenation is preferential when 2-octanol is reacted over In_2O_3. Therefore, α-hydrogen is readily extracted on In_2O_3, compared to the extraction of α-OH.

It is reported that ZrO_2 exhibits high activity for dehydration of 2-alcohol to produce olefins rather than dehydrogenation to produce ketone [35]. It is speculated that extraction of α-hydrogen is difficult over ZrO_2 that has acid–base property rather than redox property. Consequently, both reactions depicted in Fig. 7 depend on the surface property. In the present study, however, there is a difference between the formation rate of unsaturated alcohols from diols and that of butanal from 1-butanol. This indicates that there is a difference in active sites of In_2O_3 between for diols and for 1-butanol (primary alcohol).

In the reaction of 1,4-butanediol, product distribution over In_2O_3 is quite similar to that of CeO_2: 3-buten-1-ol, THF, and γ-butyrolactone are produced [7]. However, there is a difference: γ-butyrolactone is the major by-product over In_2O_3 while THF is the major by-product over CeO_2 [6,7]. On the other hand, over cubic Yb_2O_3 that has the same crystal structure as In_2O_3, the dehydrogenated products such as γ-butyrolactone are not formed [8]. This is a significant difference in the catalytic behavior between In_2O_3 and Yb_2O_3. In addition, no 4-heptanone was detected from 1-butanol over In_2O_3 in the present study, although ketonization of 1-butanol proceeds to produce 4-heptanone over CeO_2 [36,37].

In the reaction of 1,4-butanediol, dehydration to unsaturated alcohol is the main reaction, and the formation rate of unsaturated alcohol is much higher than that of butanal from 1-butanol (Fig. 6). It is speculated that the difference is attributed by the adsorption strength between the surface and the alcohols. An OH group is abstracted, while the other OH group is anchored on the surface.

Fig. 8A depicts a proposed adsorption model of 1,4-butanediol on In_2O_3: an OH group and β-hydrogen of diol are abstracted through dehydration and the other OH group acts as an anchor to the surface. In the Section 4.1, we discussed crystal structure of cubic bixbyite In_2O_3: a lot of In^{3+} are exposed at the oxygen defects of (2 2 2) plane (Fig. 5D). Fig. 8B illustrates a proposed reaction scheme: two OH groups and a β-hydrogen of diols are adsorbed on In^{3+} of the sites with tridentate coordination. During the reaction, unsaturated alcohol is produced with extracting hydrogen through redox cycle of either In^{3+}–In^{2+} or In^{3+}–In^{+}.

5. Conclusions

Vapor-phase catalytic reactions of several alcohols were investigated over In_2O_3. In the dehydration of terminal diols, such as 1,4-butanediols and 1,5-pentanediol, unsaturated alcohols were produced over In_2O_3: 3-buten-1-ol was produced with selectivity over 70 mol%, together with by-products of γ-butyrolactone and tetrahydrofuran, and 4-penten-1-ol was also produced with selectivity over 70 mol%. In_2O_3 shows stable catalytic activity for the reactions. However, in the dehydration of 1,3-diols, such as 1,3-propanediol and 1,3-butanediol, the catalytic activity of In_2O_3 was deactivated with time on stream because of carbon deposition caused by the aldehydes formed from retro aldol addition of the dehydrogenated products. In the reaction of monoalcohols over In_2O_3, such as 1-butanol and 2-octanol, dehydrogenation predominantly proceeded to produce butanal and 2-octanone, respectively.

In_2O_3 had cubic bixbyite crystal structure that is the same as those of heavy REOs. However, the catalytic activity of In_2O_3 was similar to that of cubic fluorite CeO_2 with redox property, rather than those of heavy REOs with acid–base property. In_2O_3 had redox property rather than acid–base nature. Although In_2O_3 was neutral by measuring TPD of adsorbed NH_3 and CO_2, In_2O_3 had redox property since it was reduced by hydrogen in the TPR measurement.

Oxygen defects regularly exist over the most stable In_2O_3 (2 2 2) plane (Fig. 5D), and a large number of In^{3+} are exposed on the center. Judging from the product distribution in the present reactions, it is probable that a β-hydrogen and OH groups of 1,4-butanediol adsorb on the three In^{3+} and they are abstracted as a water via the proposed redox scheme over In_2O_3, as shown in Fig. 8B.

References

[1] S. Sato, R. Takahashi, T. Sodesawa, N. Honda, H. Shimizu, Catal. Commun. 4 (2003) 77–81.
[2] S. Sato, R. Takahashi, T. Sodesawa, N. Honda, J. Mol. Catal. A 221 (2004) 177–183.
[3] N. Ichikawa, S. Sato, R. Takahashi, T. Sodesawa, J. Mol. Catal. A 231 (2005) 181–189.
[4] N. Ichikawa, S. Sato, R. Takahashi, T. Sodesawa, H. Fujita, T. Atoguchi, A. Shiga, J. Catal. 239 (2006) 13–22.
[5] A. Igarashi, N. Ichikawa, S. Sato, R. Takahashi, T. Sodesawa, Appl. Catal. A 300 (2006) 50–57.
[6] M. Kobune, S. Sato, R. Takahashi, J. Mol. Catal. A 279 (2008) 10–19.
[7] S. Sato, R. Takahashi, T. Sodesawa, N. Yamamoto, Catal. Commun. 5 (2004) 397–400.
[8] A. Igarashi, S. Sato, R. Takahashi, T. Sodesawa, M. Kobune, Catal. Commun. 8 (2007) 807–810.
[9] S. Sato, R. Takahashi, T. Sodesawa, A. Igarashi, H. Inoue, Appl. Catal. A 328 (2007) 109–116.
[10] S. Sato, R. Takahashi, N. Yamamoto, E. Kaneko, H. Inoue, Appl. Catal. A 334 (2008) 84–91.
[11] H. Inoue, S. Sato, R. Takahashi, Y. Izawa, H. Ohno, K. Takahashi, Appl. Catal. A 352 (2009) 66–73.
[12] S. Sato, R. Takahashi, M. Kobune, H. Inoue, Y. Izawa, H. Ohno, K. Takahashi, Appl. Catal. A 356 (2009) 64–71.
[13] S. Sato, R. Takahashi, M. Kobune, H. Gotoh, Appl. Catal. A 356 (2009) 57–63.
[14] B.H. Davis, J. Catal. 52 (1978) 435–444.
[15] B.H. Davis, J. Catal. 61 (1980) 279–281.
[16] A.J. Lundeen, R.V. Hoozer, J. Org. Chem. 32 (1967) 3386–3389.
[17] J.M. Trillo, S. Bernal, J. Catal. 66 (1980) 184–190.
[18] B.H. Davis, S.N. Russell, P.J. Reucroft, R.B. Shalvoy, J. Chem. Soc., Faraday Trans. I 76 (1980) 1917–1922.
[19] I. Aso, M. Nakao, N. Yamazoe, T. Seiyama, J. Catal. 57 (1979) 287–295.
[20] K. Otsuka, A. Mito, S. Takenaka, I. Yamanaka, Int. J. Hydrogen Energy 26 (2001) 191–194.
[21] T. Umegaki, K. Kuratani, Y. Yamada, A. Ueda, N. Kuriyama, T. Kobayashi, Q. Xu, J. Power Sources 179 (2008) 566–570.
[22] H. Lorenz, W. Jochum, B. Klötzer, M. Stöger-Pollach, S. Schwarz, K. Pfaller, S. Penner, Appl. Catal. A 347 (2008) 34–42.
[23] J.S. Jeong, J.Y. Lee, C.J. Lee, S.J. An, G.-C. Yi, Chem. Phys. Lett. 384 (2004) 246–250.
[24] D.R. Lide (Ed.), Handbook of Chemistry and Physics, 82nd ed., CRC Press, Boca Raton, FL, 2001.
[25] S. Sato, K. Koizumi, F. Nozaki, J. Catal. 178 (1998) 264–274.
[26] N. Ichikawa, S. Sato, R. Takahashi, T. Sodesawa, Catal. Commun. 6 (2005) 19–22.
[27] N. Yamamoto, S. Sato, R. Takahashi, K. Inui, J. Mol. Catal. A 243 (2006) 52–59.
[28] T. Nakayama, N. Ichikuni, S. Sato, F. Nozaki, Appl. Catal. A 158 (1997) 185–199.
[29] JCPDS card #06-0416.
[30] Z.L. Wang, X. Feng, J. Phys. Chem. B 107 (2003) 13563–13566.
[31] M.P. Rosynek, Catal. Rev.: Sci. Eng. 16 (1977) 111–154.
[32] G. Adachi, N. Imanaka, Chem. Rev. 98 (1998) 1479–1514.
[33] G. Adachi, N. Imanaka, Z.C. Kang, Binary Rare Earth Oxides, Kluwer Academic Publishers, 2004.
[34] D. Calestani, M. Zha, A. Zappettini, L. Lazzarini, L. Zanotti, Chem. Phys. Lett. 445 (2007) 251–254.
[35] S. Chokkaram, B.H. Davis, J. Mol. Catal. A 118 (1997) 89–99.
[36] S. Sato, R. Takahashi, T. Sodesawa, K. Matsumoto, Y. Kamimura, J. Catal. 184 (1999) 180–188.
[37] Y. Kamimura, S. Sato, R. Takahashi, T. Sodesawa, M. Fukui, Chem. Lett. (2000) 232–233.